Development of Hybrid "Fluid Jet / Float" Polishing Process.

Anthony T. H. Beaucamp*[a], Yoshiharu Namba[a], Richard R. Freeman[b]
[a]Dept. of Precision Engineering, Chubu University, Kasugai, Aichi, Japan
[b]Dept. of Research and Development, Zeeko LTD, Coalville, Leicestershire, United Kingdom

ABSTRACT

On one hand, the "float polishing" process consists of a tin lap having many concentric grooves, cut from a flat by single point diamond turning. This lap is rotated above a hydrostatic bearing spindle of high rigidity, damping and rotational accuracy. The optical surface thus floats above a thin layer of abrasive particles. But whilst surface texture can be smoothed to ~0.1nm rms (as measured by atomic force microscopy), this process can only be used on flat surfaces. On the other hand, the CNC "fluid jet polishing" process consists of pumping a mixture of water and abrasive particles to a converging nozzle, thus generating a polishing spot that can be moved along a tool path with tight track spacing. But whilst tool path feed can be moderated to ultra-precisely correct form error on freeform optical surfaces, surface finish improvement is generally limited to ~1.5nm rms (with fine abrasives). This paper reports on the development of a novel finishing method, that combines the advantages of "fluid jet polishing" (i.e. freeform corrective capability) with "float polishing" (i.e. super-smooth surface finish of 0.1nm rms or less). To come up with this new "hybrid" method, computational fluid dynamic modeling of both processes in COMSOL is being used to characterize abrasion conditions and adapt the process parameters of experimental fluid jet polishing equipment, including: (1) geometrical shape of nozzle, (2) position relative to the surface, (3) control of inlet pressure. This new process is aimed at finishing of next generation X-Ray / Gamma Ray focusing optics.

Keywords: Ultra-Precision, Finishing, Optics, X-ray, Gamma Ray, Fluid Jet Polishing, Float Polishing, Hybrid Process.

1. INTRODUCTION

Hard X-rays are emitted by extremely high energy celestial events, including supernova explosions, destruction of positrons, creation of black holes, as well as the decay of radioactive matter in space. When dealing with high energy radiations, there exists a relationship between the surface roughness of an optical surface and the upper limit of radiation energy it can reflect (measured in keV) and resolution of image it can produce (measured in arcsec). The state-of-the-art in aspheric surface finishing can produce optics with a roughness of 0.5nm rms or less, which has enabled the fabrication of soft X-ray imaging telescopes (such as ASCA [1], XMM-Newton [2] and Suzaku [3]).

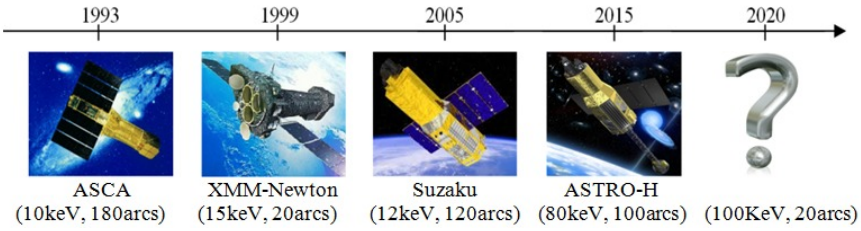

Figure 1: Past and future telescopes equipped with Wolter Type-1 imaging optics.

In recent years, research has concentrated on the development of a fabrication chain for hard X-ray telescopes (such as ASTRO-H [4]), for which the roughness specification is less than 0.3nm rms. Looking forward into the future, imaging requirements up-to 200 keV and 10 arcsec would involve finishing optical surfaces down to a roughness of 0.1nm rms or less. There is currently no finishing method that can produce large aspheric surfaces to such standard of smoothness. This paper is reporting on the initial stage of a 2 year research project funded by JSPS, that proposes to understand the mechanics of two existing finishing processes, through the application of computational fluid dynamics and experimental validation of the models (with digital pressure sensor arrays and polishing experiments), to then develop a new "hybrid" finishing method capable of finishing aspheric surfaces down to 0.1nm rms or less.

* email: beaucamp@isc.chubu.ac.jp; phone: +81-80-2239-4188

Optical Manufacturing and Testing X, edited by Oliver W. Fähnle, Ray Williamson,
Dae Wook Kim, Proc. of SPIE Vol. 8838, 88380P · © 2013 SPIE
CCC code: 0277-786X/13/$18 · doi: 10.1117/12.2023919

1.1 Float Polishing Process

The process called "float polishing" [5] consists of a tin lap cut from flat with a single point diamond tool to generate concentric grooves of 1mm in pitch and 0.3mm in depth, on top of which there are finer grooves 0.1mm in pitch. This lap is rotated with a hydrostatic bearing spindle of high rigidity, damping and rotational accuracy (see Fig. 2-left). The optical surface thus floats above a thin layer of nano-sized abrasive particles, which can smooth the surface down to 0.1nm rms (as measured by atomic force microscopy). It is however important to note that this process can only produce flat surfaces. And while the polishing effect is thought to be entirely mechanical, there has not yet been any in-depth study published on the precise conditions of the removal mechanism.

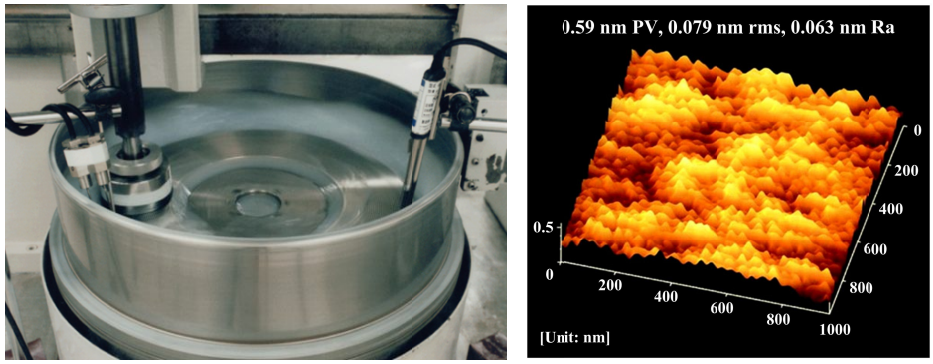

Figure 2: Float polishing machine and atomic force microscope measurement of polished Silicon surface.

1.2 Fluid Jet Polishing Process

The second process is a sub-aperture CNC controlled method called "fluid jet polishing" [6]. It consists of pumping a mixture of water and abrasive particles to a converging nozzle pointing at the optical surface (see Fig. 3-right). As the jet impinges the surface, it generates a polishing spot which is moved along a tool path with tight track spacing. The CNC machine can be controlled to correct the global form error of the work-piece. Recent developments, including modeling by finite element analysis, have permitted to improve the stability of this process and the surface roughness it delivers close to 1.0nm rms [7]. This process is currently used as an intermediate finishing step on aspheric surfaces, between diamond turning and final smoothing, for removal of diamond turning marks.

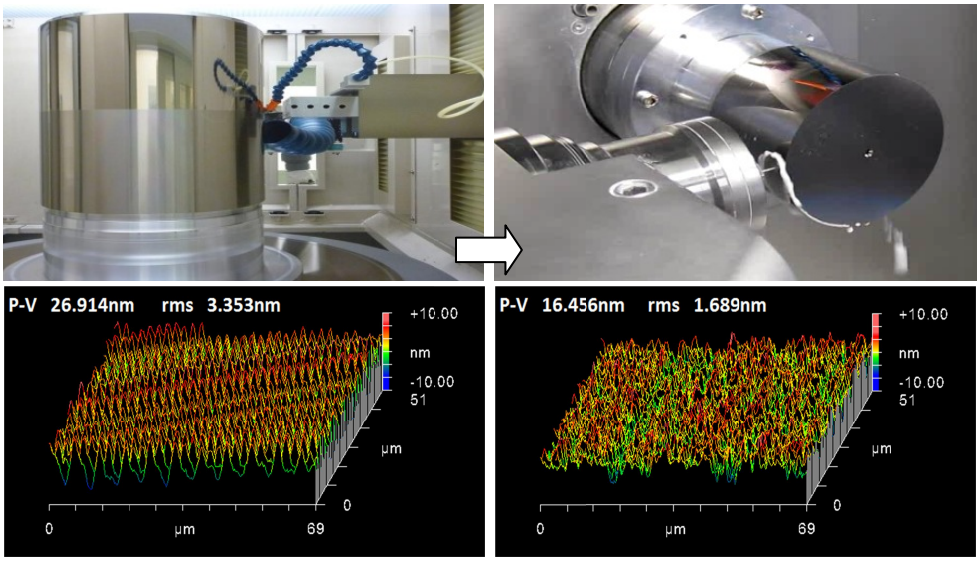

Figure 3: Surface texture of diamond turned electroless nickel before (left) and after (right) fluid jet polishing.

1.3 Development of Hybrid Process

This research paper proposes to understand the removal mechanism of these two finishing processes, through the application of computational fluid dynamics in COMSOL. After completion of this validation phase, the models will be used to research and develop a new "hybrid" finishing method capable of replicating float polishing "like" super-smooth roughness (0.1nm rms or less) on large aspheric surfaces (see Fig. 4). This will involve adapting the process condition of the fluid jet polishing equipment, including: (1) the geometrical shape of the nozzle, (2) its position relative to the surface, (3) dynamic control of the inlet pressure, such that the removal conditions of float polishing are replicated. In future, experimental validation of the models with digital pressure sensor arrays and polishing experiments will be carried out (in this paper, only simulation and optimization of process parameters are discussed).

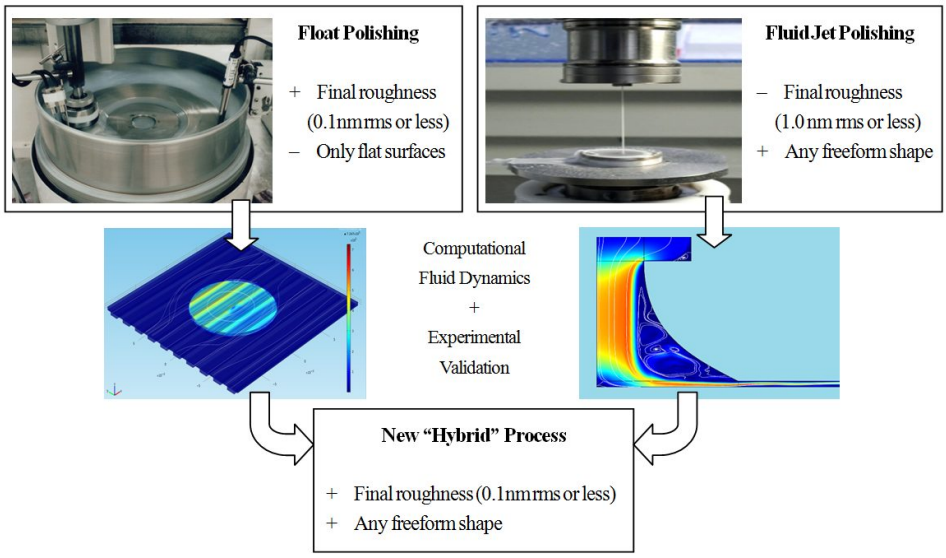

Figure 4: Proposed plan for a novel "Hybrid" finishing process.

2. NUMERICAL METHODOLOGY

2.1 Fluid Flow Description

Soares et al. [8] published a 2D model of float polishing, in which they demonstrated the ability of samples to float above the lap. In this paper, a 3D model of float polishing based on the Navier-Stokes equations is proposed. Since both float polishing and fluid jet polishing operates at relatively low pressures, and slurry temperature is stabilized externally, the assumption can be made that fluid density remains mostly constant inside these systems. The incompressible form of the Navier-Stokes equations can be used in such case to describe the fluid velocity field:

$$\rho\left(\frac{\partial \mathrm{v}}{\partial \mathrm{t}} + \mathrm{v}.\nabla \mathrm{v}\right) = -\nabla \mathrm{p} + \mu\nabla^2 \mathrm{v} + \mathrm{f}$$

where v (m/s) is the fluid velocity field, p (Pa) the fluid pressure, ρ (kg/m3) the fluid density, μ (Pa.s) the fluid viscosity, and f (N) represents external forces acting on the fluid.

2.2 Turbulence Modeling

In order to simulate the laminar to turbulent flow transition taking place at the nozzle outlet and around the floating sample, the shear-stress transport k-ω model is added to the problem. Various studies have shown the superior performance of this model compared with the k-ε model [9] when dealing with strong adverse pressure gradients. This model effectively blends the k-ω model in the near wall region with the k-ε model in the far field. A complete formulation of the model by Menter can be readily found in the literature [10].

2.3 Particle Tracing

After computing the fluid flow, a study of the motion of particles within the slurry can be carried out. For particles with mass m, the trajectory p(t) can be derived from Newton's second law of motion:

$$m\frac{\partial^2 p}{\partial t^2} = F$$

where m is the particle's mass, and F the sum of forces acting on the particle.
The external forces acting on a particle are comprised of gravitation, buoyancy, drag, and collisions with other particles. It is assumed that particle collisions cancel each other out across the entire fluid domain. And because of the high fluid velocity, it is assumed that gravitation, buoyancy, and collisions are all small compared with the drag force. The drag force can be calculated from Rayleigh's equation:

$$F = \rho C_D v^2 \frac{A}{2}$$

where ρ is the density of the fluid, C_D the drag force coefficient (inversely proportional to the Reynolds number), v the velocity relative to the fluid, and A the projected area of the particle.

2.4 Model Geometry

In the case of float polishing, the model geometry needed to be described in 3 dimensions to make accurate predictions. Because of the large dimensions of the lap compared to the samples, it was possible to simplify the lap as a linear grooved profile swept along a 3rd axis (see Fig 5). Above this swept profile, a cylindrical shape is superimposed to represent the floating sample, with transverse velocity assigned to its boundaries.

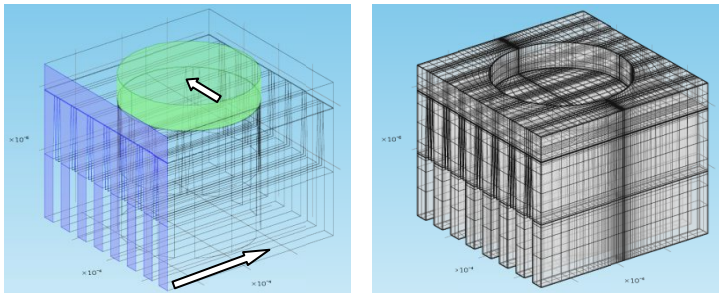

Figure 5: Float polishing: (left) simulated geometry, (right) finite element mesh.

In the case of fluid jet polishing, the model geometry consisted of a nozzle sending an impinging jet along the local normal of a flat surface. In such case, the axis of symmetry along the center of the jet makes it possible to simplify the simulation down to a 2D axi-symmetric problem (see Fig 6). The conditions of this simple case can also be easily replicated in the laboratory, using a CNC machine equipped with FJP technology.

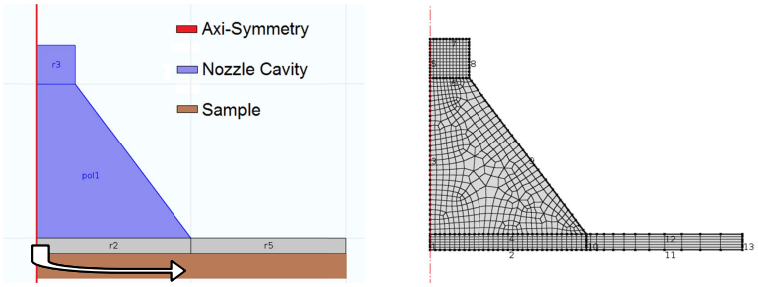

Figure 6: Fluid jet polishing: (left) simulated geometry, (right) finite element mesh.

3. SIMULATIONS AND DISCUSSION

3.1 Float Polishing

The aims of the float polishing simulations were first to establish the gap height for a given experimental situation (3mm height x 10mm diameter sample), and then derive the distribution curves of velocity and attack angle for abrasive particles colliding with the sample surface.

3.1.1 Gap Height

The height of the gap between the tin lap and floating sample was an unknown quantity. In order to derive this parameter, fluid pressure was integrated across the sample surface for a range of simulated gap values (see Fig. 7). This upward force was then compared with the downward force exerted by gravity on the sample mass. For the simulated case (6 silicon pucks of dimensions 3mm height x 10mm diameter, collectively attached to a 700g sample holder) the gap height was estimated to be around 1.5um.

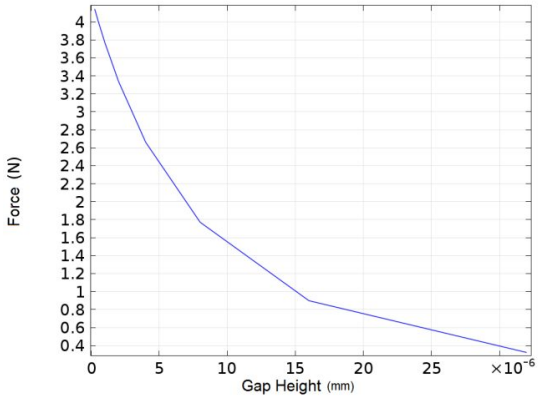

Figure 7: Force exerted by fluid pressure against sample as function of gap height.

3.1.2 Particle Velocity Distribution

Next, a simulation was run for the gap height calculated in the previous section in order to derive the pressure and velocity fields across the entire domain (see Fig. 8). Using particle tracing, the trajectories of individual abrasive particles (7nm SiO2) within the fluid stream could then be evaluated.

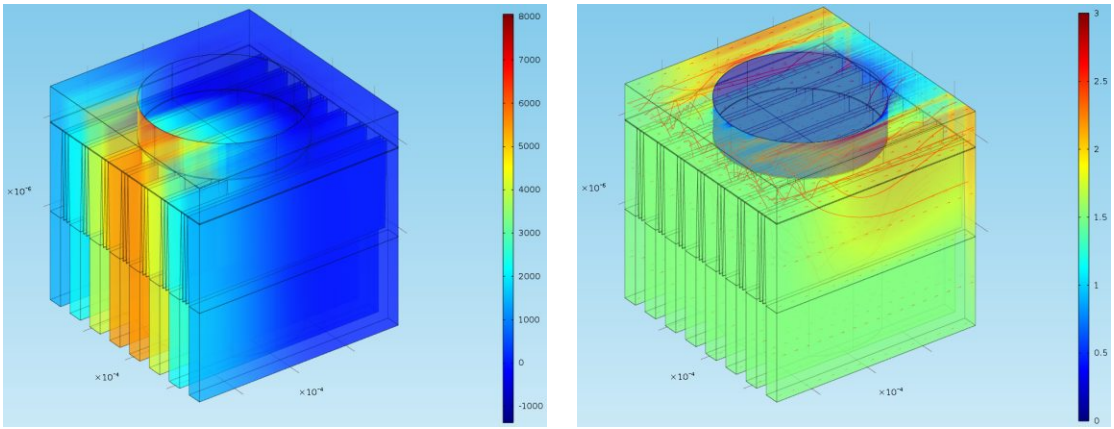

Figure 8: Pressure (left) and velocity (right) fields of fluid in float polishing simulation (particle trajectories in red).

By recording particle collisions across the sample surface, it was then possible to produce distribution curves of abrasive particle impact properties (velocity, attack angle) as shown in Fig. 9. These distribution curves (referred to as DCFP)

could then be used to optimize the process conditions of the fluid jet polishing process, in order to replicate the removal conditions of the float polishing process.

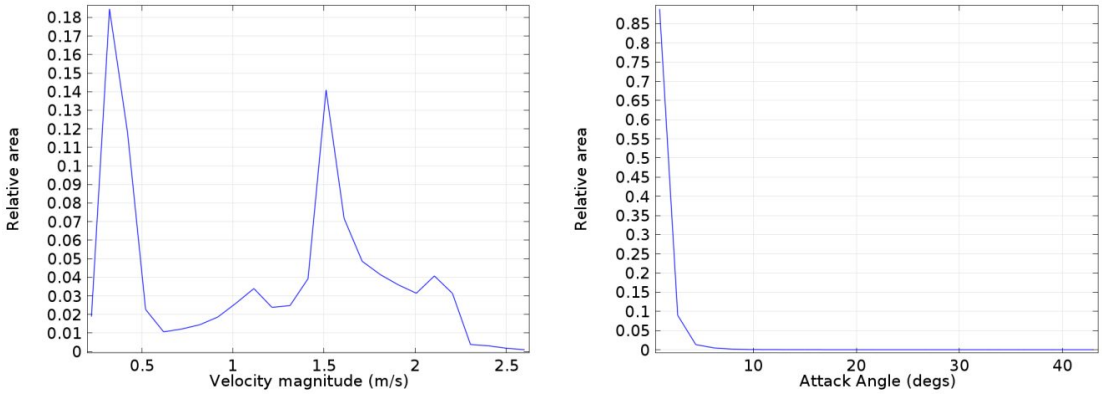

Figure 9: Velocity magnitude (left) and attack angle (right) of abrasive particles colliding with the sample surface.

3.2 Fluid Jet Polishing

The aim of the fluid jet polishing simulations was to establish which combination of nozzle geometry and process parameters (pressure, stand-off distance) could best replicate the distribution curves of abrasive particles velocity and attack angle observed in the float polishing simulation.

3.2.1 Optimization Parameters

A range of nozzle cavity geometries were simulated, including cylindrical, conical, spherical and grooved, as well as horn shapes as suggested in a previous publication by Booij et al. [11] (see Fig. 10). In each case, the pressure and gap distance were varied across a range of values, to derive the pressure and velocity fields. Using particle tracing, abrasive particles velocities and attack angle across the sample surface were derived (referred to as DCJFP). The optimization cost function consisted of the RMS of the difference between DCFP and DCFJP distributions.

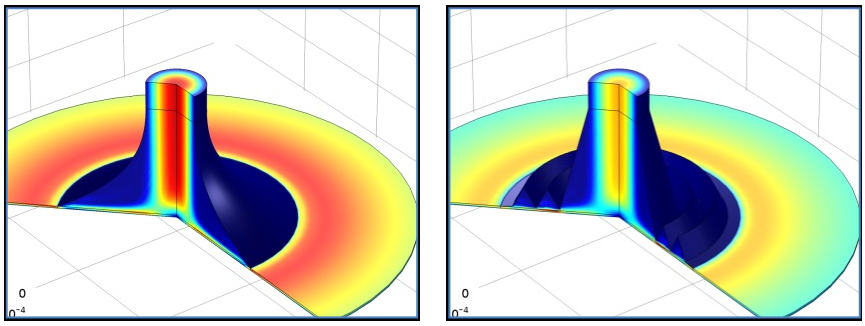

Figure 10: Some of the cavity geometries simulated during the optimization exercise: horn (left) and grooved shaped (right).

3.2.2 Optimization Results

In the case of single compartment cavities (cylinder, cone, sphere and horn), it was found that escape velocities were generally similar for a given inlet pressure and nozzle stand-off distance. By contrast, the float polishing velocity distribution curve (Fig. 9) featured two separate velocity spikes (corresponding respectively to the lap velocity and sample traverse speed). It was found that by designing a grooved cavity, and optimizing the width and location of each groove, the double spiked velocity histogram could be replicated. By further optimizing the fluid pressure and nozzle gap distance, a good match between the distribution curves DCFP and DCFJP could be obtained (see Fig. 11).

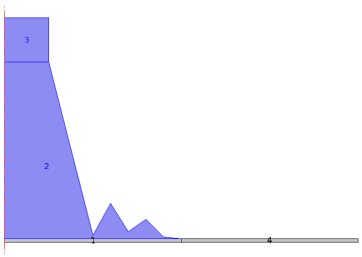

Figure 11: Grooved nozzle cavity design derived from optimization.

4. CONCLUSION

In this paper, a 3D model of the float polishing process was proposed, and used to determine the fluid gap height under specific process conditions. Particle tracing was then used to establish the distribution curves (DCFP) of velocity and attack angle of the abrasive particles, as they collide with the floating sample surface.
The DCFP distribution curves were then used to optimize the parameters of fluid jet polishing simulations. Different nozzle cavity geometries and process conditions were simulated, until the FJP distribution curves (DCFJP) matched the conditions observed for float polishing as best as possible. It was found that a grooved cavity, with optimum width and position values for each groove, provided the best match between DCFP and DCFJP.
The next step will involve experimental verification of the optimized process, by fabricating custom nozzles and testing them on various substrates prepared by lapping. This future research is expected to result in the development of a new finishing process for super-smoothing large aspheric optics to less than 0.1nm rms. By pushing forward the state-of-the-art and enabling the fabrication of optical components capable of focusing hard X-ray radiations with energy up-to 200 keV and resolution of 10 arcsec, it is hoped that this research will open the door for new scientific discoveries in both astrophysics and particle physics.

ACKNOWLEDGMENTS

This work is supported by a Grant-in-Aid for Scientific Research (B) No. 22360063 and also by the Postdoctoral Fellowship Program for Foreign Researchers, from the Japan Society for the Promotion of Science.

REFERENCES

[1] http://www.isas.jaxa.jp/e/enterp/missions/asca/
[2] http://xmm.vilspa.esa.es/
[3] http://www.astro.isas.ac.jp/suzaku/
[4] http://astro-h.isas.jaxa.jp/
[5] Namba Y., Ohnishi N., Yoshida S., Harada K. and Yoshida K., “Ultra-Precision Float Polishing of Calcium Fluoride Single Crystals for Deep Ultra Violet Applications”, Annals of CIRP, Vol. 53/1, pp. 459-462 (2004).
[6] Beaucamp A., Namba Y., "Super-smooth finishing of diamond turned hard X-ray molding dies by combined fluid jet and bonnet polishing", CIRP Annals-Manufacturing Technology (2013).
[7] Beaucamp A., Freeman R., Namba Y., “Dynamic Multiphase Modeling and Optimization of Fluid Jet Polishing Process”, Annals of the CIRP, Vol. 61/1 (2012).
[8] Soares S. F., Baselt D. R., Black J. P., Jungling K. C. and Stowell W. K., “Float-polishing process and analysis of float-polished quartz“, Applied optics, Vol. 33/1, pp. 89-95 (1994).
[9] Yu Y., Liu X., Wu J., Meng H., “Comparison among Turbulence Models for a Novel Static Circulating Jet Mixer”, AMM, Vol. 26/28, pp. 382 (2010).
[10] Menter, Z., “Two-Equation Eddy-Viscosity Turbulence Models for Engineering Applications”, AIAA Journal, Vol. 32/8, pp. 1598-1605 (1994).
[11] Booij S., Faehnle O., Meeder M., Wons T. and Braat J., "Jules Verne: a new polishing technique related to FJP", In Optical Science and Technology, SPIE 48th Annual Meeting, pp. 89-100 (2004).